

# Anomalous vibrational dispersion in holographically trapped colloidal arrays

Marco Polin and David G. Grier

*Department of Physics and Center for Soft Matter Research, New York University, New York, NY 10003*

Stephen R. Quake

*Department of Bioengineering, Stanford University, Palo Alto, CA 94305*

(Dated: January 26, 2006)

Colloidal spheres localized in an array of harmonic wells form a thermally excited, viscously damped dynamical system capable of supporting propagating elastic waves. Experimentally realized with micrometer-scale polystyrene spheres localized in a line of holographic optical traps, the hydrodynamically coupled array's behavior is quantitatively explained by a model based on the Oseen superposition approximation. The spheres' purely dissipative coupling is predicted to mediate a crossover to a regime of underdamped propagating elastic waves with uniformly negative group velocities that has yet to be verified experimentally.

PACS numbers: 87.80.Cc, 82.70.Dd, 05.60.Cd

The many-body dynamics of driven dissipative systems often are governed by hydrodynamic coupling. Even in the simplest systems, this can lead to interesting and unexpected behavior. For example, Meiners and Quake [1] demonstrated that the thermally driven fluctuations of two non-interacting colloidal spheres individually localized in the harmonic potential wells of two optical tweezers are strongly anticorrelated at short times and small separations. Cooperative motion in this case is a consequence of the hydrodynamic forces the spheres exert on each other as they relax into their respective potential wells. Its appearance suggests that an extended system of independently trapped hydrodynamically coupled spheres might behave as an elastic medium, and that the spheres' predilection for anticorrelated motion might give rise to unusual time-dependent properties.

This Letter describes an experimental and theoretical study of thermally driven vibrations in a one-dimensional hydrodynamically coupled colloidal crystal created with the holographic optical trapping technique [2–4]. Each sphere is localized in an individual optical tweezer [5], and the spheres interact only through their influence on the surrounding viscous medium. We show experimentally that the normal modes of such a dissipatively coupled solid are consistent with a Langevin-Oseen model. This theory further predicts that elastic waves can propagate in this system despite the absence of conservative interactions. These waves exhibit anomalous dispersion and negative group velocities as a generic feature.

Related phenomena have been studied in dusty plasmas whose highly charged constituent particles can be harmonically constrained in one or two dimensions by external electric fields [6–9], and in charge-stabilized colloidal crystals [10, 11]. The present system differs from these and most other solids in that cooperativity arises from the spatial dependence of a purely dissipative interaction. Negative group velocities also distinguish the optical properties of cold atomic gases and certain semi-

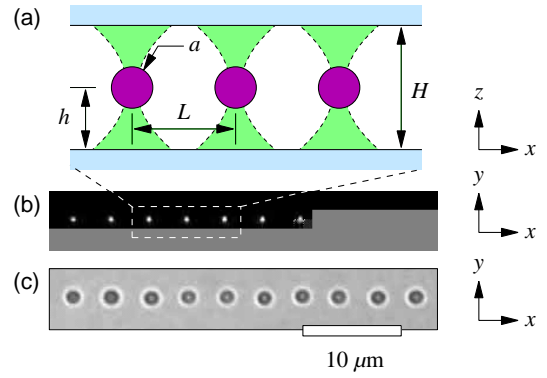


FIG. 1: (a) Holographically trapped array of colloidal spheres dispersed in a viscous fluid. (b) Focused light from an array of traps at  $L = 2.6 \mu\text{m}$ . (c) Colloidal polystyrene spheres  $1.48 \mu\text{m}$  in diameter trapped in the array at  $h = H/2$ .

conducting systems, where they result from resonances.

Our experimental setup is sketched in Fig. 1(a). We create arrays of uniformly strong optical tweezers by imprinting computer-generated holograms [4] onto the wavefronts of a  $\lambda = 532 \text{ nm}$  laser beam (Coherent Verdi) with a liquid crystal spatial light modulator (SLM) (Hamamatsu X7550 PAL-SLM). The modified beam is focused into an array of traps with a  $100\times$ , NA 1.4, SPlan Apo oil immersion objective lens mounted in a Zeiss S100TV Axiovert inverted optical microscope. Placing a front-surface mirror on the microscope's stage allows us to photograph the focused trap array, as in Fig. 1(b). Photometry on such images confirms that the traps' intensities vary by less than 5 percent from the mean, and thus that their trapping characteristics should be comparably uniform [4].

The traps are projected into a sample of colloidal polystyrene spheres  $2a = 1.48 \pm 0.14 \mu\text{m}$  in diameter (Bangs Labs Lot number 6064) dispersed in a 75 percent (w/w) mixture of glycerol (Fisher Scientific Lot number

04377) in deionized water. Allowing the dispersion to equilibrate in air reduces the screening length to less than 300 nm [12, 13] and effectively eliminates electrostatic interactions among the spheres. Adding 1 mM NaCl reduces the screening length to 12 nm without affecting the results that follow. The sample is sealed within a slit pore  $H = 32 \mu\text{m}$  thick formed by bonding the edges of a #1 cover glass to a microscope slide, and the traps are focused to the midplane,  $h = H/2$ , to minimize hydrodynamic coupling of the spheres to the walls.

We regulate the sample's temperature, and thus its viscosity by heating from above with a transparent indium-tin-oxide heater whose temperature is fixed to  $T = 40.00 \pm 0.05^\circ\text{C}$  by a Lake Shore 330 temperature controller. Thermal contact with the microscope objective at  $T = 22^\circ\text{C}$  establishes a vertical temperature gradient, with the temperature at the trapping plane estimated to be  $T = 35.3 \pm 0.2^\circ\text{C}$ . Under these conditions, the solution should have a viscosity of  $\eta = 17 \text{ mPa}\cdot\text{s}$ , which corresponds to a free-sphere viscous drag coefficient of  $\gamma = 6\pi\eta a = 0.24 \text{ pN}\cdot\text{s}/\mu\text{m}$ . Evaporation of water during sample preparation, however, can increase this substantially, and we instead measure  $\gamma$  *in situ*.

Figure 1(c) shows a typical video frame of ten spheres trapped in the array. Experiments were performed with center-to-center separations ranging from  $L = 2.6 \mu\text{m}$  to  $L = 3.7 \mu\text{m}$ , which are large enough to avoid artifacts due to overlapping images [14]. Standard methods of digital video analysis [15] allow us to track the spheres' centroids in the plane with 6 nm resolution at 1/30 sec intervals. With an estimated 3 mW of light per trap, the particles' thermally driven root mean-squared (RMS) displacements are around  $\sigma = 50 \text{ nm}$ . Tracking individual spheres over 5 minutes allows us to characterize both the traps' potential wells and the particles' viscous drag coefficients [4]. The traps are accurately described as symmetric harmonic wells in the plane with a stiffness of  $k = 0.993 \pm 0.087 \text{ pN}/\mu\text{m}$ . The uncertainty here is comparable to the single-trap measurement error [4] of  $\Delta k/k = 0.077$ , with additional contributions coming from a combination of the measured differences in the traps' intensities and the 2.2 percent variation in these spheres' diameters inferred from measurements of  $\gamma$ . The extracted value,  $\gamma = 0.46 \pm 0.01 \text{ pN}\cdot\text{s}/\mu\text{m}$ , is consistent with an 81.6 percent (w/w) glycerol concentration. The associated viscous relaxation time,  $\tau = \gamma/k = 460 \pm 40 \text{ msec}$ , exceeds the video sampling interval of 33 msec sufficiently that the array's dynamics can be captured by conventional digital video analysis.

The particles' measured trajectories were decomposed into the normal modes anticipated for hydrodynamically coupled spheres. We compute these using Faxén's law [16] in the approximation that a particle at location  $\mathbf{r}_n$  is advected by the flow field  $\mathbf{u}(\mathbf{r}_n)$  generated by its neighbors. In the absence of other interactions, a system of  $N$  identical spheres of radius  $a$  at positions  $\{\mathbf{r}_n\}$  responds

to a set of forces  $\{\mathbf{F}_n\}$  by moving with velocities  $\{\mathbf{v}_n\}$  dictated by the  $N$ -body Oseen tensor  $\mathbf{H}_{i,j}$

$$\mathbf{v}_i = \sum_{j=1}^N \mathbf{H}_{i,j} \mathbf{F}_j. \quad (1)$$

Assuming that the spheres are well localized in traps at  $\mathbf{R}_n = nL\hat{\mathbf{x}}$ , with  $L \gg a$ , we may approximate  $\mathbf{H}_{i,j}$  by the pairwise superposition of stokeslets [17],

$$\mathbf{H}_{i,j} \approx \frac{\mathbf{I}}{\gamma} \delta_{i,j} + \frac{3}{4\gamma} \frac{a}{r_{ij}} (\mathbf{I} + \hat{\mathbf{r}}_{ij} \otimes \hat{\mathbf{r}}_{ij}) (1 - \delta_{i,j}), \quad (2)$$

where  $\mathbf{r}_{ij} = \mathbf{r}_i - \mathbf{r}_j$ ,  $r_{ij} = |\mathbf{r}_{ij}|$ , and  $\mathbf{I}$  is the identity tensor. This approximation has proved effective in previous experimental studies of colloidal hydrodynamics [1, 18–20]. If we further assume that the spheres' fluctuations about their equilibrium positions are much smaller than their mean separation,  $L$ , we may replace  $\mathbf{r}_i$  with  $\mathbf{R}_i$  in Eq. (2) to obtain a time-independent approximation to  $\mathbf{H}_{i,j}$ . The Langevin equation for the  $i$ -th sphere is then

$$m \frac{d^2 \mathbf{r}_i}{dt^2} = -k [\mathbf{r}_i(t) - \mathbf{R}_i] - \sum_{j=1}^N \mathbf{H}_{i,j}^{-1} \frac{d\mathbf{r}_j}{dt} + \mathbf{f}_i(t), \quad (3)$$

where  $m$  is the sphere's mass and  $\mathbf{f}_i(t)$  describes the thermal forces acting on the sphere. For a system in equilibrium at temperature  $T$ ,  $\langle \mathbf{f}_i(t) \rangle = 0$  and

$$\langle \mathbf{f}_i(t) \mathbf{f}_j(t') \rangle = 2k_B T \mathbf{H}_{i,j}^{-1} \delta(t - t'), \quad (4)$$

where  $k_B$  is Boltzmann's constant. Retaining the inertial term in Eq. (3) enables us investigate conditions under which the optically trapped array admits propagating modes.

The Oseen tensor can be decomposed into longitudinal ( $\parallel$ ) and transverse ( $\perp$ ) components relative to the array's axis,  $\hat{\mathbf{x}}$ . The associated normal modes,  $\xi_i^\parallel(t)$  and  $\xi_i^\perp(t)$ , are eigenvectors of the matrices

$$(\gamma \mathbf{H}^\parallel)_{ij} = \begin{cases} 1, & i = j \\ \frac{3}{2} \frac{a}{L} \frac{1}{|i-j|}, & i \neq j \end{cases} \quad \text{and} \quad (5)$$

$$(\gamma \mathbf{H}^\perp)_{ij} = \begin{cases} 1, & i = j \\ \frac{3}{4} \frac{a}{L} \frac{1}{|i-j|}, & i \neq j \end{cases}. \quad (6)$$

Measured trajectories are combined accordingly.

The eigenvalue  $\lambda_j$  associated with the normal mode  $\xi_j$  in a particular polarization describes that mode's time evolution through the  $N$ -body Langevin equation

$$m \frac{d^2 \xi_j}{dt^2} = -k \xi_j - \frac{\gamma}{\lambda_j} \frac{d\xi_j}{dt} + \Phi_j(t), \quad (7)$$

where the thermal forcing terms  $\{\Phi_j\}$  are Gaussian random variables with zero mean and covariance

$$\langle \Phi_i(t) \Phi_j(t') \rangle = 2 \frac{k_B T \lambda_i}{\gamma} \delta_{i,j} \delta(t - t'). \quad (8)$$

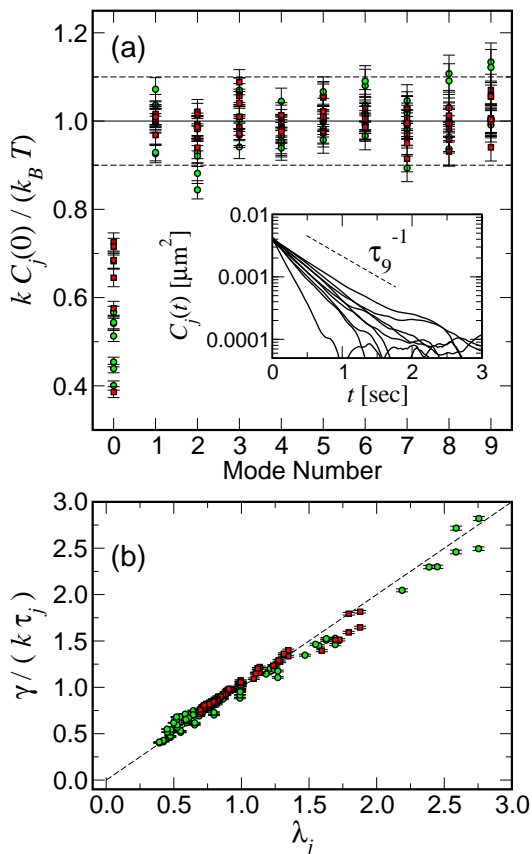


FIG. 2: Variance (a) and decay rates (b) for normal modes in seven separate experiments at lattice constants ranging from  $L = 2.6 \mu\text{m}$  to  $3.7 \mu\text{m}$ , compared with predictions based on superposition of pairwise hydrodynamic interactions in the stokeslet approximation. Longitudinal modes are plotted as (green) circles and transverse modes as (red) squares. The inset to (a) shows typical time-dependent autocorrelations for the longitudinal modes at  $L = 2.6 \mu\text{m}$ .

Accordingly, solutions to Eq. (7) in the limit of strong damping satisfy

$$\langle \xi_j(t) \xi_j(0) \rangle = C_j(0) e^{-t/\tau_j}, \quad (9)$$

where the variance,  $C_j(0) = k_B T/k$ , and the relaxation time,  $\tau_j = \gamma/(k\lambda_j)$ , completely characterize the motion.

The success of this description can be gauged from comparisons with data in Fig. 2. Normal mode fluctuations were recorded for 20 minutes at each of seven different lattice constants ranging from  $L = 2.6 \mu\text{m}$  to  $L = 3.7 \mu\text{m}$ . Both the normal modes and their associated eigenvalues are determined solely by the geometric ratio  $a/L$ , and the data were analyzed accordingly. As expected for a thermally equilibrated system obeying equipartition, the normal modes' normalized covariances,  $kC_j(0)/(k_B T)$ , plotted in Fig. 2(a) collapse to unity to within 10 percent, independent of lattice constant. The common mode (mode 0) departs from unity due to its extreme sensitivity to slow instrumental drifts. Its offset

from the other modes in all seven runs is consistent with a random drift of 70 nm over 10 minutes. The other normal modes are more robust against such artifacts, and their variances are consistent with the measured differences in the traps' intensities. The inverse autocorrelation times plotted in Fig. 2(b) also agree with calculated eigenvalues, thereby confirming the correct decomposition of the particles' motions into normal modes. Successful collapse of the data over a range of interparticle separations also helps to rule out any effect of electrostatic interactions.

Having verified the model's accuracy in this range of parameters, we can now comment more generally on the nature of vibrational waves' propagation in this class of systems. From Eq. (7), the frequency associated with the  $j$ -th normal mode is

$$\frac{\omega_j}{\omega_0} = \sqrt{1 - g_j^2} + i g_j, \quad (10)$$

where  $\omega_0^2 = k/m$  and  $g_j = \gamma/(2m\omega_0 \lambda_j)$ . For the present system,  $\omega_0 = 1.6 \times 10^4 \text{ sec}^{-1}$ . We recast Eq. (10) as a dispersion relation for elastic waves by associating a wavenumber with each mode. For an infinite array, translation invariance implies eigenmodes of the form

$$\mathbf{r}_n(q) = A(q) \hat{\mathbf{n}} \exp(\pm i n L q), \quad (11)$$

with wavenumbers  $q \in [0, \pi/L)$ , amplitudes  $A(q)$  and polarization vectors  $\hat{\mathbf{n}} = \hat{\mathbf{x}}$  or  $\hat{\mathbf{y}}$ . The associated eigenvalues are

$$\lambda^{\parallel}(q) = 1 - 3 \frac{a}{L} \ln \left( 2 \sin \frac{qL}{2} \right) \quad \text{and} \quad (12)$$

$$\lambda^{\perp}(q) = 1 - \frac{3}{2} \frac{a}{L} \ln \left( 2 \sin \frac{qL}{2} \right). \quad (13)$$

Substituting these into Eq. (10) yields the dispersion relations,  $\omega^{\parallel}(q)$  and  $\omega^{\perp}(q)$ , for longitudinal and transverse elastic waves, respectively. Wavenumbers may be associated with the eigenmodes of the finite system by fitting sinusoids to the eigenvectors of  $\gamma \mathbf{H}$ .

Figure 3 shows representative data from Fig. 2, obtained at  $L = 2.8 \mu\text{m}$ , replotted as the imaginary branch of a dispersion relation. The results agree quantitatively with Eqs. (10), (12) and (13), which are shown as dashed curves. The absence of propagating modes in such a highly damped system is not surprising. Diverging eigenvalues at longer wavelengths, however, guarantee a crossover to real-valued eigenfrequencies and thus to propagating modes for *any* values of  $k$ ,  $\gamma$  and  $m$ , even when the single-sphere Reynolds number is small. The crossover to real dispersion can be moved into the experimentally accessible realm by trapping larger spheres more rigidly in a lower-viscosity medium, as shown by the solid curves in Fig. 3. Under all conditions,  $\text{Re}\{\omega(q)\}$  decreases monotonically with  $q$  so that the propagating excitations all have negative group velocities. Both the crossover to underdamped wave propagation and also

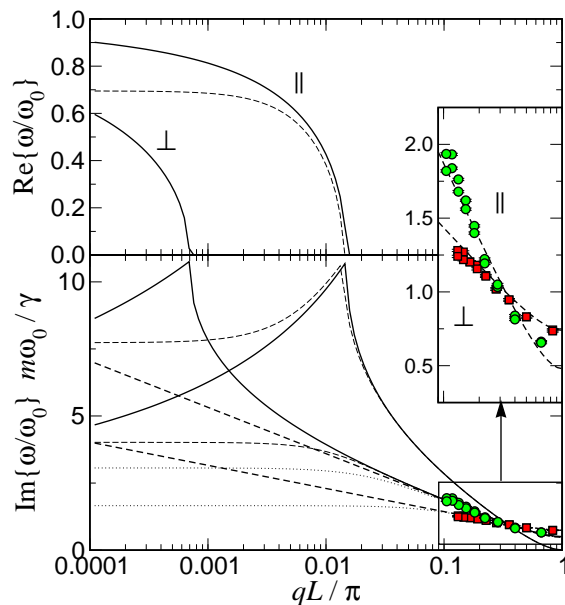


FIG. 3: Real and imaginary parts of the dispersion relation for hydrodynamically coupled arrays of spheres. Discrete points show measurements at  $L = 2.8 \mu\text{m}$  together with predictions of Eqs. (10), (12) and (13) (dashed curves). The crossover to propagating modes (solid curves) is computed for  $3 \mu\text{m}$  diameter silica spheres dispersed in acetaldehyde at room temperature in traps with stiffness  $k = 30 \text{ pN}/\mu\text{m}$ . Dotted curves include hydrodynamic coupling to a surface at  $h = 16 \mu\text{m}$ .

these modes' anomalous dispersion arise not from direct inter-particle interactions as in other systems, but rather from the separation dependence of the viscous damping.

In practice, hydrodynamic coupling to bounding surfaces tends to suppress long-wavelength propagating modes. Accounting for these in the stokeslet approximation [17, 21] (dotted curves in Fig. 3) yields no measurable change in the predicted dispersion for our experimental conditions, and no qualitative change for the predicted crossover to propagating longitudinal modes.

A crossover from overdamped to underdamped dynamics at large wavelengths has been predicted [10] and recently observed [11] for the transverse lattice vibrations of colloidal crystals. This crossover, however, is governed by direct inter-particle interactions rather than by hydrodynamic coupling. Colloidal crystals consequently exhibit normal dispersion for transverse waves in the propagating regime, and their longitudinal modes are always overdamped. The hydrodynamically coupled lattice, by contrast, supports propagating modes with anomalous dispersion in both polarizations.

Underdamped elastic waves propagate in dusty plasmas, with no crossover to overdamped dynamics [8, 9]. The plasma medium has low enough viscosity that hydrodynamic coupling between neighboring particles is negligible. Here again, confining the spheres to one or two dimensions with externally imposed potentials in-

duces anomalous dispersion for waves polarized along the confined directions [8, 9]. In this case, however, negative group velocities result from the interplay of confining potentials and the particles' electrostatic interactions. Spheres in the present system, by contrast, interact only through their influence on the viscous medium, with propagating modes vanishing at low viscosity. Optically organized arrays of noninteracting spheres in viscous fluids therefore constitute a distinct class of elastic media whose ability to transmit elastic waves is a consequence of dissipation instead of conservative interactions.

We thank Paul Chaikin and John Goree for helpful discussions. This work was supported by the National Science Foundation under Grant Number DMR-0451589.

- 
- [1] J.-C. Meiners and S. R. Quake, Phys. Rev. Lett. **82**, 2211 (1999).
  - [2] E. R. Dufresne and D. G. Grier, Rev. Sci. Instr. **69**, 1974 (1998).
  - [3] J. E. Curtis, B. A. Koss, and D. G. Grier, Opt. Comm. **207**, 169 (2002).
  - [4] M. Polin, K. Ladavac, S.-H. Lee, Y. Roichman, and D. G. Grier, Opt. Express **13**, 5831 (2005).
  - [5] A. Ashkin, J. M. Dziedzic, J. E. Bjorkholm, and S. Chu, Opt. Lett. **11**, 288 (1986).
  - [6] S. V. Vladimirov, P. V. Shevchenko, and N. F. Cramer, Phys. Rev. E **56**, R74 (1997).
  - [7] G. Piacente, F. M. Peeters, and J. J. Betouras, Phys. Rev. E **70**, 036406 (2004).
  - [8] T. Misawa, N. Ohno, K. Asano, M. Sawai, S. Takamura, and P. K. Kaw, Phys. Rev. Lett. **86**, 1219 (2001).
  - [9] B. Liu, K. Avinash, and J. Goree, Phys. Rev. Lett. **91**, 255003 (2003).
  - [10] A. J. Hurd, N. A. Clark, R. C. Mockler, and W. J. O'Sullivan, Phys. Rev. A **26**, 2869 (1982).
  - [11] B. V. R. Tata, P. S. Mohanty, M. C. Valsakumar, and J. Yamanaka, Phys. Rev. Lett. **93**, 268303 (2004).
  - [12] C. S. Miner and N. N. Dalton, *Glycerol* (Reinhold, New York, 1953).
  - [13] J. N. Butler *Carbon Dioxide Equilibria and Their Application* (Addison-Wesley, London, 1982).
  - [14] J. Baumgartl and C. Bechinger, Europhys. Lett. **71**, 487 (2005).
  - [15] J. C. Crocker and D. G. Grier, J. Colloid Interface Sci. **179**, 298 (1996).
  - [16] J. Happel and H. Brenner, *Low Reynolds Number Hydrodynamics* (Kluwer, Dordrecht, 1991).
  - [17] C. Pozrikidis, *Boundary Integral and Singularity Methods for Linearized Viscous Flow* (Cambridge University Press, New York, 1992).
  - [18] J. Crocker, J. Chem. Phys. **106**, 2837 (1997).
  - [19] E. R. Dufresne, T. M. Squires, M. P. Brenner, and D. G. Grier, Phys. Rev. Lett. **85**, 3317 (2000).
  - [20] E. R. Dufresne, D. Altman, and D. G. Grier, Europhys. Lett. **53**, 264 (2001).
  - [21] A. J. Hurd, N. A. Clark, R. C. Mockler, and W. J. O'Sullivan, J. Fluid Mech. **153**, 401 (1985).